

We are IntechOpen, the world's leading publisher of Open Access books Built by scientists, for scientists

6,900

Open access books available

186,000

International authors and editors

200M

Downloads

Our authors are among the

154

Countries delivered to

TOP 1%

most cited scientists

12.2%

Contributors from top 500 universities



WEB OF SCIENCE™

Selection of our books indexed in the Book Citation Index
in Web of Science™ Core Collection (BKCI)

Interested in publishing with us?
Contact book.department@intechopen.com

Numbers displayed above are based on latest data collected.
For more information visit www.intechopen.com



Copper, Iron, and Aluminium Electrochemical Corrosion Rate Dependence on Temperature

Mykhaylo Viktorovych Yarmolenko

Abstract

Our investigations show that electrochemical corrosion of copper is faster than electrochemical corrosion of aluminium at temperatures below 100°C. Literature data analysis shows that the Al atoms diffuse faster than the Cu atoms at temperatures higher than 475°C, Al-rich intermetallic compounds (IMCs) are formed faster in the Cu-Al system, and the Kirkendall plane shifts towards the Al side. Electrochemical corrosion occurs due to electric current and diffusion. An electronic device working time, for example, depends on the initial copper cover thickness on the aluminium wire, connected to the electronic device, temperature, and volume and dislocation pipe diffusion coefficients, so copper, iron, and aluminium electrochemical corrosion rates are investigated experimentally at room temperature and at temperature 100°C. Intrinsic diffusivities ratios of copper and aluminium at different temperatures and diffusion activation energies in the Cu-Al system are calculated by the proposed methods here using literature experimental data. Dislocation pipe and volume diffusion activation energies of pure iron are calculated separately by earlier proposed methods using literature experimental data. Aluminium dissolved into NaCl solution as the Al^{3+} ions at room temperature and at temperature 100°C, iron dissolved into NaCl solution as the Fe^{2+} (not Fe^{3+}) ions at room temperature and at temperature 100°C, copper dissolved into NaCl solution as the Cu^+ ions at room temperature, and as the Cu^+ and the Cu^{2+} ions at temperature 100°C. It is found experimentally that copper corrosion is higher than aluminium corrosion, and the ratio of electrochemical corrosion rates, $k_{\text{Cu}}/k_{\text{Al}} > 1$, decreases with temperature increasing, although iron electrochemical corrosion rate does not depend on temperature below 100°C. It is obvious because the melting point of iron is higher than the melting point of copper or aluminium. It is calculated that copper electrochemical corrosion rate is approximately equal to aluminium electrochemical corrosion at a temperature of about 300°C, so the copper can dissolve into NaCl solution mostly as the Cu^{2+} ions at a temperature of about 300°C. The ratio of intrinsic diffusivities, $D_{\text{Cu}}/D_{\text{Al}} < 1$, increases with temperature increasing, and intrinsic diffusivity of aluminium could be approximately equal to intrinsic diffusivity of copper at a temperature of about 460°C.

Keywords: electrochemical corrosion, metallic coatings, electrolysis, diffusion, intermetallic compounds, phases formation kinetics, copper, aluminium, iron, Kirkendall-Frenkel porosity, Kirkendall shift, activation energy

1. Introduction

An Al wire coated with a thin Cu cover ($\approx 15\text{-}\mu\text{m}$ thickness), utilised near an automobile motor, is heated to temperatures about 373–473 K (100–200°C). Intermetallics (IMCs) can be formed at the Cu/Al interface and grow gradually during heating at such temperatures. The IMC layers are brittle and have high resistivity. Therefore, for assurance of the reliability of the product, information on the growth behaviour of the IMC layers during heating is essentially important [1]. **Figure 1** shows the problem: an electronic device working time, t_0 , depends on initial Cu cover thickness, X_{Cu} , and temperature. The electric conductivity of copper is higher than the electric conductivity of aluminium in approximately two times, but the formation of intermetallic phases induces a significant increase in contact resistance, which is found to increase linearly with the thickness of the intermetallics formed [2]. The temperature range used to produce the intermetallic phases was from 250 to 515°C. Moreover, the presence of an electrical field greatly accelerated the kinetics of formation of intermetallic phases and altered significantly their morphology, and the impaired mechanical integrity of the Al-Cu bimetallic joints treated by an electrical current was clearly demonstrated by an extensive cracking not only across the whole intermetallic bandwidth but also within different phases and at a neighbouring interface [2]. Three-phase thickness, X_{123} , can be estimated in such a way. The mass conservation law gives

$$X_{Cu}(t=0) \cdot 1 = \frac{9}{9+4}X_3(t_0) + \frac{1}{1+1}X_2(t_0) + \frac{1}{1+2}X_1(t_0) \approx \frac{1.526X_{123}}{3} \approx 0.509X_{123}, \text{ and } X_{123} \approx 2X_{Cu}, \quad (1)$$

so three-phase general thickness is approximately greater in two times than the initial Cu cover thickness.

Otherwise, it was proved experimentally that a thin Al pad ($\approx 1\text{-}\mu\text{m}$ thickness) can prevent gold and copper corrosion because the intermetallics formation rate in Au-Al system is much higher than the intermetallic formation rate in Cu-Al system, so it is possible to use Cu instead of Au for wire bonding in microelectronic packaging, and Cu has higher electric conductivity, higher thermal conduction, and

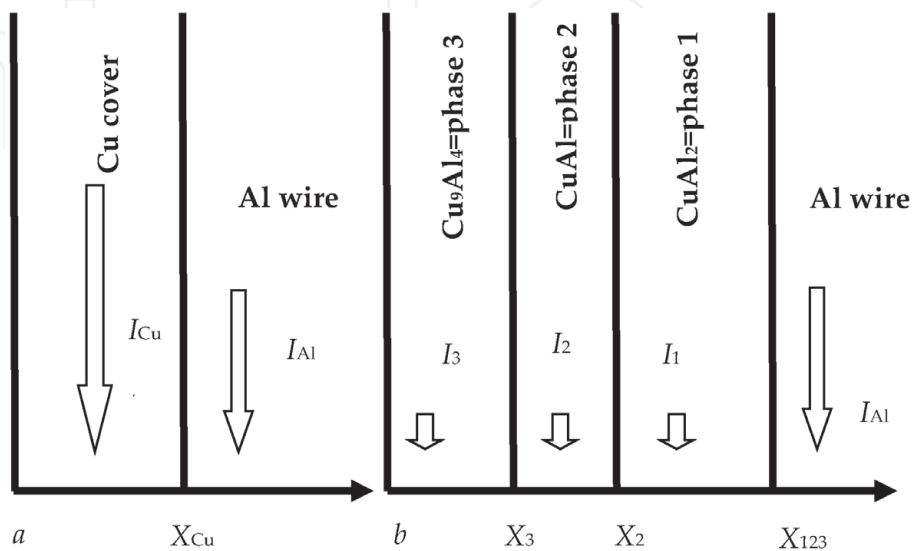


Figure 1.

(a) Initial stage ($t = 0$): An electronic device is working, since the electric current, $I_a = I_{Cu} + I_{Al}$, has optimal value; (b) final stage ($t = t_0$): The electronic device is not working, because the electric current, $I_b = I_3 + I_2 + I_1 + I_{Al}$, has too small value, since pure Cu cover has disappeared.

lower material cost than Au [3]. Corrosion and intermetallic rate formation in gold and copper wire bonding in microelectronics packaging were investigated in [3] at temperatures $T_1 = 175^\circ\text{C}$, $T_2 = 200^\circ\text{C}$, and $T_3 = 225^\circ\text{C}$ during 120, 240, 360, and 480 h. The authors have reported that cross-sectional analysis of the Cu ball on Al pad confirmed that corrosion occurred at temperatures about $T = 200^\circ\text{C}$ primarily beneath the Cu balls and did not initiate from the Al pad, formation of CuCl_2 did not allow self-passivation of Cu to occur, so the rate of copper corrosion increased, and the rate of Cu-Al intermetallics formation was found to be three to five times slower than Au-Al intermetallic formation at all three annealing temperatures. So, copper dissolved into NaCl solution as Cu^{2+} ions at temperatures about $T = 200^\circ\text{C}$, as we expected. They did not investigate corrosion rate dependence of copper and aluminium on temperature. Moreover, phase layers general thicknesses for Cu-Al system were calculated [3]:

$$\begin{aligned} X_{123}^2 &= K_{123}t + K_{01} = K_0 e^{-Q/(RT)} + K_{01} \\ &= 3.52 \cdot 10^{-4} \mu\text{m}^2/\text{s} \cdot e^{-25500\text{Jmol}^{-1}/(RT)} t + 0.44 \mu\text{m}^2, \end{aligned} \quad (2)$$

where $R \approx 8.314 \text{ JK}^{-1}$ is the gas constant, and K_{01} is the constant related to initial IMC thickness. General reaction rates of IMC formation were calculated: $K_{123}(T_1) = 3.57 \cdot 10^{-7} \mu\text{m}^2/\text{s}$, $K_{123}(T_2) = 6.26 \cdot 10^{-7} \mu\text{m}^2/\text{s}$, and $K_{123}(T_3) = 7.15 \cdot 10^{-7} \mu\text{m}^2/\text{s}$. The pre-exponential factor and IMC formation activation energy was calculated: $K_0 \approx 3.52 \cdot 10^{-4} \mu\text{m}^2/\text{s}$, $Q \approx 25.5 \text{ kJ/mol}$. We can use these results to calculate the electronic device working time by Eq. (14) in [4] at different temperatures:

$$t_0 \approx \frac{X_{\text{Cu}}^2}{C_3 K_{123}} = \frac{169}{81} \frac{X_{\text{Cu}}^2}{K_{123}} \approx \frac{2X_{\text{Cu}}^2}{K_0} e^{Q/(RT)} \approx 5900 \cdot X_{\text{Cu}}^2 [\mu\text{m}^2] \cdot e^{25.5\text{kJmol}^{-1}/(RT)} \text{s}; \quad (3)$$

$$t_0(T_1 = 175^\circ\text{C} = 448\text{K}) \approx 5900 \cdot 225 \cdot e^{25500/(8.314 \cdot 448)} \text{s} \approx 40\text{years};$$

$$t_0(T_2 = 200^\circ\text{C}) \approx 28\text{years};$$

$$t_0(T_3 = 225^\circ\text{C}) \approx 21\text{years}; t_0(T_4 = 300^\circ\text{C}) \approx 9\text{years}; t_0(T_5 = 350^\circ\text{C}) \approx 6\text{years}.$$

Other researchers have obtained [5]: $K_{123}(T_4 = 300^\circ\text{C}) = 4.2 \cdot 10^{-4} \mu\text{m}^2/\text{s}$, $K_{123}(T_5 = 350^\circ\text{C}) = 3.4 \cdot 10^{-3} \mu\text{m}^2/\text{s}$. Eq. (3) gives

$$t_0(T_4 = 300^\circ\text{C}) \approx \frac{2X_{\text{Cu}}^2}{K_{123}} \approx 12\text{days}; t_0(T_5 = 350^\circ\text{C}) \approx \frac{2X_{\text{Cu}}^2}{K_{123}} \approx 1.5\text{days}.$$

We can calculate: $Q \approx 124 \text{ kJ/mol}$; $K_0 \approx 8.5 \cdot 10^{-5} \text{ m}^2/\text{s} = 8.5 \cdot 10^7 \mu\text{m}^2/\text{s}$;

$$t_0(T = 175^\circ\text{C}) \approx 5.3 \cdot 10^{-6} \cdot e^{124\text{Jmol}^{-1}/(448\text{K})} \text{s} \approx 49\text{years}; t_0(T = 200^\circ\text{C}) \approx 8.4\text{years};$$

$$t_0(T = 225^\circ\text{C}) \approx \frac{2X_{\text{Cu}}^2}{K_0} e^{Q/(RT)} \approx 5.3 \cdot 10^{-6} \cdot e^{124\text{Jmol}^{-1}/(498\text{K})} \text{s} \approx 1.7\text{years}.$$

It was reported in [1] that the growth of layer 1 is controlled predominantly by boundary diffusion, but that of layers 2 and 3 are governed mainly by volume diffusion at temperatures $T = 483\text{--}543 \text{ K}$ ($210\text{--}270^\circ\text{C}$) for various periods up to 3.456Ms (960 h). The authors obtained: $K_{01} \approx 5.3 \cdot 10^{-7} \text{ m}^2/\text{s}$, $Q_1 \approx 86 \text{ kJ/mol}$, $K_{023} \approx 4.2 \cdot 10^{-5} \text{ m}^2/\text{s}$, $Q_{23} \approx 146 \text{ kJ/mol}$. We can calculate: $K_{123}(T_6 = 210^\circ\text{C}) = 1.5 \cdot 10^{-6} \mu\text{m}^2/\text{s}$,

$$t_0(T = 210^\circ\text{C}) \approx \frac{2X_{\text{Cu}}^2}{K_{123}} \approx 9.6\text{years}.$$

The less temperature is, the higher contribution of grain-boundary diffusion and dislocation pipe diffusion to the layers growth is, so models of grain-boundary diffusion and dislocation pipe diffusion involving outflow into volume should be taken into account [6–8].

Diffusion activation energy of Al is less than diffusion activation energy of Cu ($Q_{Al} < Q_{Cu}$) at temperatures from 160–250°C for mutual diffusion in copper-aluminium thin film double layers, but the pre-exponential factors are different in 10 times [9]:

$$D_{Al}^* = 4 \cdot 10^{-5} e^{-121kJmol^{-1}/(RT)} m^2/s, D_{Cu}^* = 9.5 \cdot 10^{-4} e^{-135kJmol^{-1}/(RT)} m^2/s, \quad (4)$$

in θ -phase (phase 1) $CuAl_2$, $C_{Al} = 2/3 \approx 0.67$, $C_{Cu} = 1/3 \approx 0.33$;

$$D_{Al}^* = 1.5 \cdot 10^{-11} e^{-68kJmol^{-1}/(RT)} m^2/s, D_{Cu}^* = 1 \cdot 10^{-6} e^{-106kJmol^{-1}/(RT)} m^2/s, \quad (5)$$

in η_2 -phase (phase 2) $CuAl$, $C_{Al} = C_{Cu} = 1/2 = 0.5$;

$$D_{Al}^* = 1.7 \cdot 10^{-7} e^{-116kJmol^{-1}/(RT)} m^2/s, D_{Cu}^* = 2.4 \cdot 10^{-6} e^{-125kJmol^{-1}/(RT)} m^2/s, \quad (6)$$

in γ_2 -phase (phase 3) Cu_9Al_4 , $C_{Al} = 4/13 \approx 0.31$, $C_{Cu} = 9/13 \approx 0.69$.

We can calculate the mutual diffusion coefficient for each phase at temperature 160°C by the Darken equation [8, 10] and taking into account Eqs. (4)–(6):

$$D_i^* = C_{Al} D_{Cu}^* + C_{Cu} D_{Al}^*; i = 1, 2, 3; D_1^* = 6.64 \cdot 10^{-20} m^2/s; D_2^* = 1.3 \cdot 10^{-19} m^2/s; D_3^* = 1.8 \cdot 10^{-21} m^2/s.$$

We can calculate using the methods described in [4, 11]: $K_{123}(T_7 = 160^\circ C) \approx 2.8 \cdot 10^{-6} \mu m^2/s$, $t_0(T = 160^\circ C) \approx \frac{2X_{Cu}^2}{K_{123}} \approx 5 \text{ years}$, so the problem remains unsolved.

It was founded experimentally, that copper electrochemical corrosion is higher than aluminium electrochemical corrosion in approximately two times at room temperature [4, 11], so a thin Al layer can prevent copper electrochemical corrosion. It was reported also about the influence of hydrogen and the absence of a passive layer on the corrosive properties of aluminium alloys [12].

Besides, the soldered copper/tin-based contacts are the weakest part of the chip that can be related to intermetallics and the Kirkendall-Frenkel porosity formation in the contact zone [13]. One of the most common reasons for chip failure is the soldered. The typical range of packaging and operation of the integrated circuits is from room temperature to 250°C [14].

Hydrostatic pressure of Argon gas (≈ 10 MPa) can decrease Kirkendall-Frenkel porosity formation, but practically cannot decrease mutual diffusion coefficients, but hot isostatic pressing ($p \approx 100$ MPa, Argon) removes porosity due to homogenisation heat treatment in alloy CMSX4 and superalloy CMSX10 [15].

It was clarified also that carbon steel-stainless steel with the environment of flowing sodium chloride does indeed produce synergetic corrosion instead of antagonistic corrosion [16].

Electric current can destruct wire bonding in microelectronics packaging, so we planned to investigate copper, iron, and aluminium electrochemical corrosion at room temperature and temperature 100°C. Direct current can dissolve metal anode into electrolyte, and we planned to do experiments under the same conditions: initial radii of Cu, Fe, and Al anodes should be approximately equal, electrolyte concentration should be the same, anodes lengths immersed into electrolyte should

be equal, graphite cathodes should be the same, direct electric current value should be practically the same. Aluminium can dissolve into electrolyte only as of the Al^{3+} ions, so the charge of aluminium ions should be exactly equal to 3, but copper can dissolve into electrolyte as the Cu^+ ions and the Cu^{2+} ions, and the charge of copper ions could be equal to 1 or 2, and iron can dissolve into electrolyte as the Fe^{2+} ions and the Fe^{3+} ions, and the charge of iron ions could be equal to 2 or 3. We need to find appropriate mathematical equations to calculate the charges of copper, iron, and aluminium ions dissolved into NaCl solution.

2. Experimental results of copper, iron, and aluminium electrochemical corrosion

2.1 Investigation at room temperature

Cylindrical anodes (99.99% Cu, 99.96% Fe, and 99.99% Al) were used for copper and aluminium [4, 11], and also iron electrochemical corrosion investigation. Sodium chloride (NaCl) solution was used as an electrolyte (Figure 2).

Direct electric current and anode mass decreasing were measured. First of all, we need to be assured that the Cu^+ ions (or the Cu^{2+}), the Fe^{2+} (or the Fe^{3+}), and the Al^{3+} were present in NaCl solution. The rate of anode dissolving into electrolyte can be calculated using Faraday's law of electrolysis:

$$\frac{dm}{dt} = \frac{MI}{zF}, dm = \rho \cdot L \cdot \pi \cdot d(R^2(t)). \tag{7}$$

Here, m is anode mass dissolved into the electrolyte, t is a time of the experiment, M is molar mass, I is the direct electric current value, F is the Faraday constant ($F \approx 96,500 \text{ C mol}^{-1}$), z is a charge of ions, R is anode radius, L is anode length immersed into the electrolyte. Electric current value did not change, so one can calculate:

$$z = \frac{MIt}{F\pi\rho L(R^2(t = 0) - R^2(t))}, \tag{8}$$

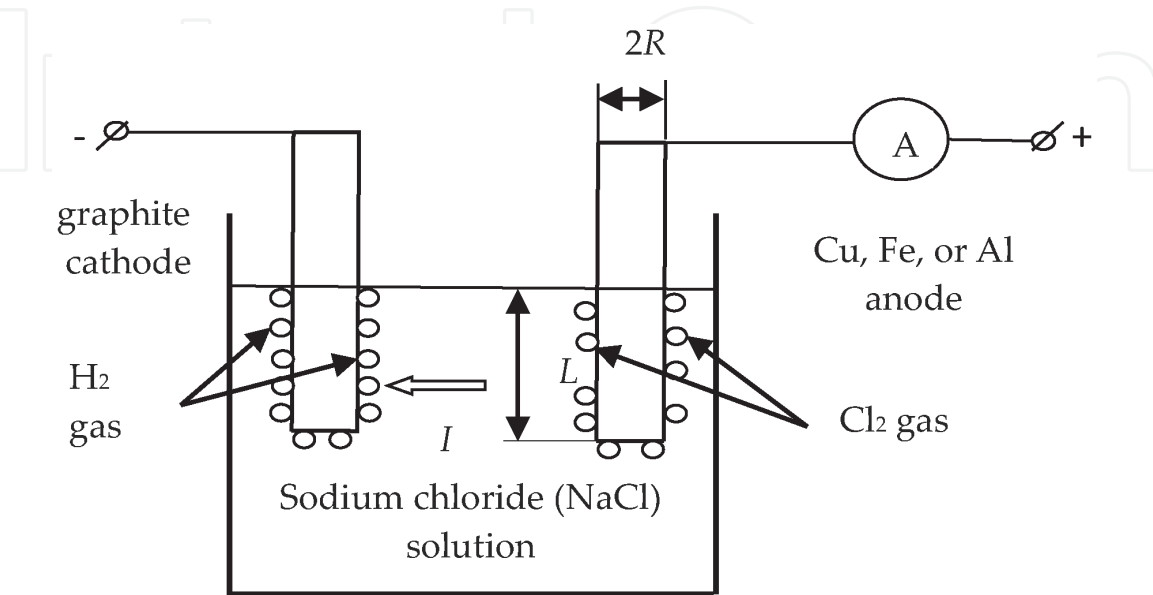


Figure 2.
Scheme of experimental equipment at room temperature. Cu, Fe, and Al anodes dissolve into NaCl solution as Cu^+ , Fe^{2+} , and Al^{3+} ions.

where ρ is anode density. Charges of copper, iron, and aluminium ions were calculated:

$$z_{Cu} = \frac{63.55 \cdot 10^{-3} \text{ kg/mol} \cdot 2.8 \text{ A} \cdot 1.2 \cdot 10^3 \text{ s}}{F \cdot \pi \cdot 8.9 \cdot 10^3 \text{ kg/m}^3 L_{Cu} \cdot (R_{Cu}^2(t=0) - R_{Cu}^2(t_4))} \approx 0.995 \approx 1, \quad (9)$$

$$z_{Al} = \frac{27 \cdot 10^{-3} \text{ kg/mol} \cdot 3.1 \text{ A} \cdot 1.2 \cdot 10^3 \text{ s}}{F \cdot \pi \cdot 2.7 \cdot 10^3 \text{ kg/m}^3 L_{Al} \cdot (R_{Al}^2(t=0) - R_{Al}^2(t_4))} \approx 2.954 \approx 3, \quad (10)$$

$$z_{Fe} = \frac{55.847 \cdot 10^{-3} \text{ kg/mol} \cdot 3.15 \text{ A} \cdot 1.2 \cdot 10^3 \text{ s}}{F \cdot \pi \cdot 7.86 \cdot 10^3 \text{ kg/m}^3 L_{Fe} \cdot (R_{Fe}^2(t=0) - R_{Fe}^2(t_4))} \approx 2.03 \approx 2, \quad (11)$$

where $L_{Cu} \approx L_{Al} \approx L_{Fe}$; $L_{Cu} = L_{Fe} = 5 \cdot 10^{-2} \text{ m}$, $L_{Al} = 4.5 \cdot 10^{-2} \text{ m}$; $R_{0Cu} = R_{0Al} = 2.8 \text{ mm}$, $R_{0Fe} = 2.98 \text{ mm}$; $I_{Al} \approx I_{Cu} \approx I_{Fe}$; $I_{Fe} = 3.15 \text{ A}$, $I_{Al} = 3.1 \text{ A}$, $I_{Cu} = 2.8 \text{ A}$, so copper dissolved into NaCl solution as the Cu^+ ions, iron dissolved into NaCl solution as the Fe^{2+} ions, and aluminium dissolved into NaCl solution as the Al^{3+} ions. Anodes radii-decreasing kinetics is shown in **Figure 3**. Experiments were carried during $t_1 = 5 \text{ min}$, $t_2 = 10 \text{ min}$, $t_3 = 15 \text{ min}$, and $t_4 = 20 \text{ min}$. Experimental results are as follows: $R_{1Cu} = 2.74 \text{ mm}$, $R_{2Cu} = 2.67 \text{ mm}$, $R_{3Cu} = 2.59 \text{ mm}$, $R_{4Cu} = 2.5 \text{ mm}$; $R_{1Al} = 2.77 \text{ mm}$, $R_{2Al} = 2.73 \text{ mm}$, $R_{3Al} = 2.68 \text{ mm}$, $R_{4Al} = 2.62 \text{ mm}$, $R_{1Fe} = 2.95 \text{ mm}$, $R_{2Fe} = 2.92 \text{ mm}$, $R_{3Fe} = 2.88 \text{ mm}$, $R_{4Fe} = 2.83 \text{ mm}$. Measurement precision was 0.01 mm or 10 micrometres.

Chemical reactions took place near the positive electrode (anode):

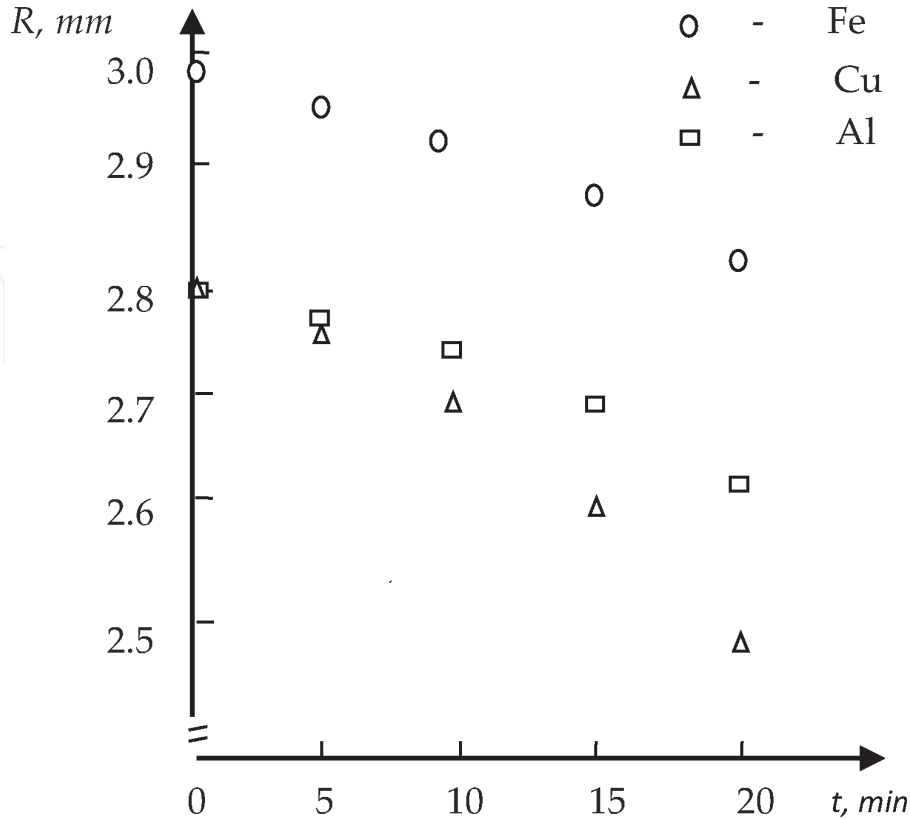
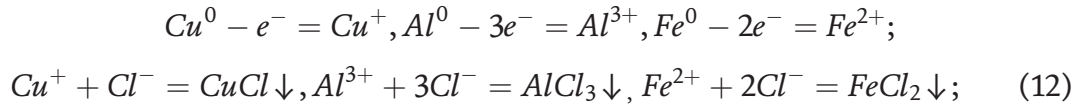
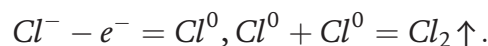
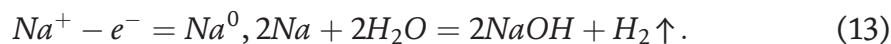


Figure 3.
Cu, Fe, and Al anodes radii decreasing kinetics at room temperature.



Chlorine gas was formed near the anode.

Chemical reactions took place near the negative electrode (cathode):



Hydrogen gas was formed near the cathode.

Anodes radii decreasing rate constants can be calculated as the average value of four experiments to increase calculation precise:

$$k_{Cu} = \frac{4R_0^2 - \sum_{i=1}^4 R_i^2}{\sum_{i=1}^4 t_i} \approx 1.25 \cdot 10^{-9} m^2/s, k_{Al} = \frac{4R_0^2 - \sum_{i=1}^4 R_i^2}{\sum_{i=1}^4 t_i} \approx 7.29 \cdot 10^{-10} m^2/s, \quad (14)$$

$$k_{Fe} = \frac{4R_{0Fe}^2 - \sum_{i=1}^4 R_{iFe}^2}{\sum_{i=1}^4 t_i} \approx 7.26 \cdot 10^{-10} m^2/s, k_{Cu} \approx 1.71k_{Al}; k_{Al} \approx k_{Fe},$$

so copper electrochemical corrosion is much higher than aluminium and iron electrochemical corrosion, despite $I_{Fe} \approx I_{Al} \geq I_{Cu}$: $I_{Fe} \approx I_{Al} \approx 1.1I_{Cu}$. It needs to point out that k_{Cu} , k_{Fe} , and k_{Al} have dimensionalities as diffusion coefficients [m^2/s], because electrochemical corrosion occurs through anodes' surface.

2.2 Investigation at temperature 100°C

Experiments were carried also at temperature 100°C. Cylindrical anodes (99.99% Cu, 99.99% Al, and 99.96% Fe) were used for copper and aluminium [17] and also iron electric corrosion investigation. Sodium chloride (NaCl) solution was used as an electrolyte (**Figure 4**). Direct electric current and anodes' mass decreasing rate were measured (**Figure 5**).

Electric current value did not change, so one can calculate the following:

$$z_{Cu} = \frac{63.55 \cdot 10^{-3} kg/mol \cdot 3.05A \cdot 1.2 \cdot 10^3 s}{F \cdot \pi \cdot 8.9 \cdot 10^3 kg/m^3 L_{Cu} \cdot (R_{Cu}^2(t=0) - R_{Cu}^2(t_4))} \approx 1.47 \approx \frac{1+2}{2}, \quad (15)$$

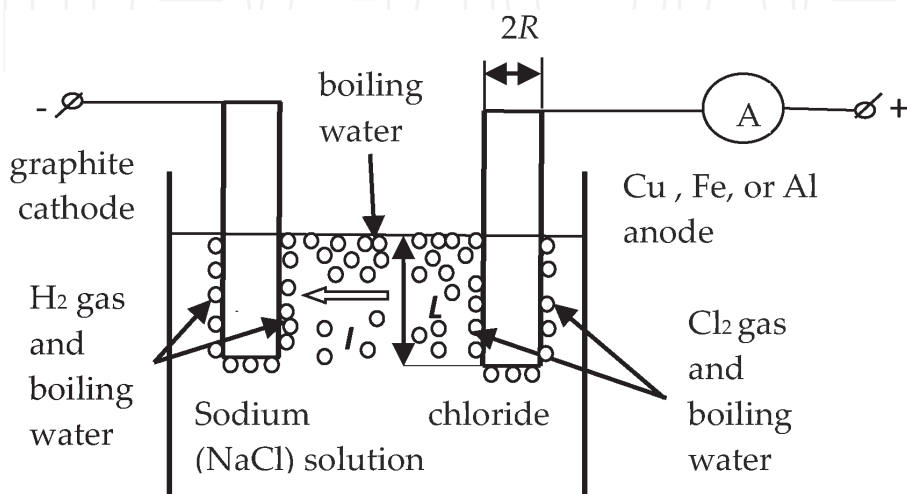


Figure 4.
Scheme of experimental equipment at $T = 100^\circ C$. Cu, Fe, and Al anodes dissolved into NaCl solution as Cu^+ , cu^{2+} , Fe^{2+} , and Al^{3+} ions.

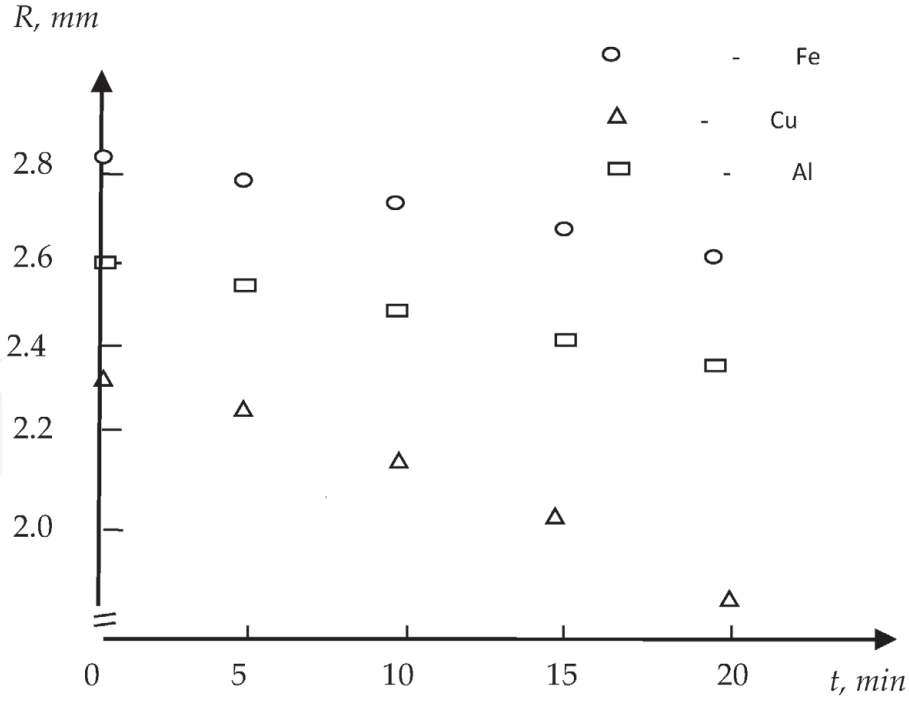


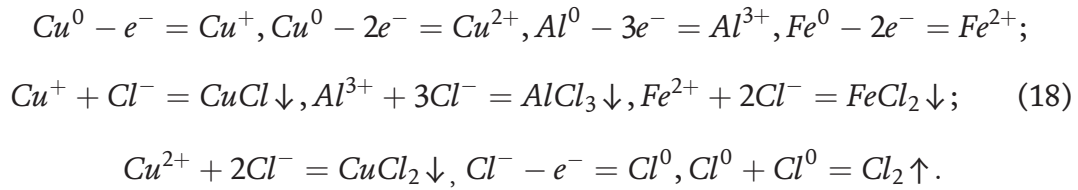
Figure 5.
Cu, Fe, and Al anodes radii decreasing kinetics at $T = 100^\circ\text{C}$.

$$z_{Al} = \frac{27 \cdot 10^{-3} \text{ kg/mol} \cdot 3.15 \text{ A} \cdot 1.2 \cdot 10^3 \text{ s}}{F \cdot \pi \cdot 2.7 \cdot 10^3 \text{ kg/m}^3 L_{Al} \cdot (R_{Al}^2(t=0) - R_{Al}^2(t_4))} \approx 2.85 \approx 3, \quad (16)$$

$$z_{Fe} = \frac{55.847 \cdot 10^{-3} \text{ kg/mol} \cdot 3.15 \text{ A} \cdot 1.2 \cdot 10^3 \text{ s}}{F \cdot \pi \cdot 7.86 \cdot 10^3 \text{ kg/m}^3 L_{Fe} \cdot (R_{Fe}^2(t=0) - R_{Fe}^2(t_4))} \approx 2.01 \approx 2, \quad (17)$$

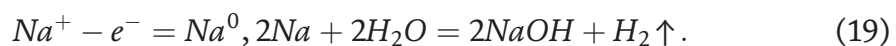
where $L_{Cu} = L_{Al} = 4 \cdot 10^{-2} \text{ m}$, $L_{Fe} = 5 \cdot 10^{-2} \text{ m}$, $R_{0Cu} = 2.27 \text{ mm}$, $R_{0Al} = 2.6 \text{ mm}$, $R_{0Fe} = 2.83 \text{ mm}$, $I_{Al} = 3.15 \text{ A}$, $I_{Fe} = 3.13 \text{ A}$, $I_{Cu} = 3.05 \text{ A}$, so copper dissolved into NaCl solution as Cu^+ and Cu^{2+} ions (copper dissolved into NaCl solution as Cu^+ ions at room temperature), iron dissolved into NaCl solution as the Fe^{2+} ions (as at room temperature), and aluminium dissolved into NaCl solution as Al^{3+} ions (as at room temperature). Anode radii-decreasing kinetics is shown in **Figure 5**. Experiments were carried during $t_1 = 5 \text{ min}$, $t_2 = 10 \text{ min}$, $t_3 = 15 \text{ min}$, and $t_4 = 20 \text{ min}$. Experimental results are as follows: $R_{1Cu} = 2.2 \text{ mm}$, $R_{2Cu} = 2.12 \text{ mm}$, $R_{3Cu} = 2.03 \text{ mm}$, $R_{4Cu} = 1.92 \text{ mm}$; $R_{1Al} = 2.56 \text{ mm}$, $R_{2Al} = 2.51 \text{ mm}$, $R_{3Al} = 2.45 \text{ mm}$, $R_{4Al} = 2.38 \text{ mm}$; $R_{1Fe} = 2.80 \text{ mm}$, $R_{2Fe} = 2.76 \text{ mm}$, $R_{3Fe} = 2.72 \text{ mm}$, $R_{4Fe} = 2.67 \text{ mm}$. Measurement precision was 0.01 mm or 10 micrometres. We carried additional experiments, but the result was the same.

Chemical reactions are more complicated at 100°C than at room temperature near positive electrodes (anodes):



Chlorine gas and boiling water were formed near anodes.

Chemical reactions took place near negative electrodes (cathodes):



Hydrogen gas and boiling water were formed near cathodes.

Anode radii-decreasing rate constants can be calculated as average value of four experiments to increase calculation precise:

$$\begin{aligned}
 k_{Cu} &= \frac{4R_{0Cu}^2 - \sum_{i=1}^4 R_{iCu}^2}{\sum_{i=1}^4 t_i} \approx 1.154 \cdot 10^{-9} m^2/s, \{1.25 \cdot 10^{-9} \text{ at room temperature}\}, \\
 k_{Al} &= \frac{4R_{0Al}^2 - \sum_{i=1}^4 R_{iAl}^2}{\sum_{i=1}^4 t_i} \approx 8.42 \cdot 10^{-10} m^2/s, \{7.29 \cdot 10^{-10} \text{ at room temperature}\}, \\
 k_{Fe} &= \frac{4R_{0Fe}^2 - \sum_{i=1}^4 R_{iFe}^2}{\sum_{i=1}^4 t_i} \approx 6.83 \cdot 10^{-10} m^2/s, \{7.23 \cdot 10^{-10} \text{ at room temperature}\}, \\
 k_{Cu} &\approx 1.37k_{Al}, \{1.72 \text{ at room temperature } T_1 \approx 27^\circ C\},
 \end{aligned}
 \tag{20}$$

so copper electrochemical corrosion is higher at room temperature $T_1 \approx 27^\circ C$, aluminium electrochemical corrosion is higher at temperature $T_2 = 100^\circ C$, and the ratio of electrochemical corrosion rates, k_{Cu}/k_{Al} , decreases with temperature increasing, although iron electrochemical corrosion rate practically does not depend on temperature below $100^\circ C$. It is obvious, because of the higher melting point of iron than the melting point of copper or aluminium. We can conclude that the Cu^{2+} ions are less mobile than Cu^+ ions. It needs to point out that k_{Cu} , k_{Al} , and k_{Fe} have dimensionalities as diffusion coefficients, D_{Cu}^* , D_{Al}^* , D_{Fe}^* [m^2/s], because electrochemical corrosion occurs through anodes' surface.

Dislocation pipe and volume diffusion activation energies can be calculated in such a way. The Arrhenius law is valid for dislocation pipe diffusion and volume diffusion in ultra-high-purity samples [8, 18]:

$$D_d^* = D_{0d}e^{-Q_d/(RT)} \text{ or } D_d^* = D_{0d}e^{-E_d/(k_B T)}, \text{ and } D_V^* = D_{0V}e^{-Q_V/(RT)} \text{ or } D_V^* = D_{0V}e^{-E_V/(k_B T)}, \tag{21}$$

$$Q [J/mol] = F \cdot E [eV]. \tag{22}$$

Here, $R \approx 8.314 \text{ JK}^{-1}$ is the gas constant, k_B is the Boltzmann constant, $Q_d(E_d)$ is the dislocation pipe diffusion activation energy ($Q_d = FE_d$), $F \approx 96,500 \text{ Cmol}^{-1}$ is the Faraday constant, $Q_V(E_V)$ is the volume diffusion activation energy ($Q_V = FE_V$), D_{0d} and D_{0V} are the pre-exponential factors, T is the absolute temperature.

Our experimental results allow us to calculate:

$$\frac{k_{Cu}}{k_{Al}}(T) \approx \frac{D_{Cu}^*}{D_{Al}^*}(T) = \frac{D_{0Cu}^*}{D_{0Al}^*} e^{(Q_{Al} - Q_{Cu})/(RT)}; \ln \left(\frac{D_{0Cu}^*}{D_{0Al}^*} \right) = -0.6; Q_{Al} - Q_{Cu} = 2.9 \text{ kJ/mol}, \tag{23}$$

$$\frac{D_{0Cu}^*}{D_{0Al}^*} = 0.55, \frac{D_{Cu}^*}{D_{Al}^*}(T_3) = 1 \Rightarrow T_3 = \frac{2900 \text{ J/mol}}{0.6R} \approx 583 \text{ K} \approx 310^\circ C, \tag{24}$$

so diffusion activation energy of Al, Q_{Al} , is higher than the diffusion activation energy of Cu, Q_{Cu} , ($Q_{Al} > Q_{Cu}$, $Q_{Al} - Q_{Cu} = 2.9 \text{ kJ/mol}$), at temperatures from 20 to $100^\circ C$, because the Cu^+ ions have higher mobilities than the Al^{3+} ions, and copper electrochemical corrosion rate can be approximately equal to aluminium electrochemical corrosion at temperature about $T_3 \approx 300^\circ C$ due to the Cu^{2+} ions are less mobile than the Cu^+ ions. Moreover, the pre-exponential factors are approximately the same: $D_{0Al}^* \approx 2D_{0Cu}^*$.

3. Intrinsic diffusivities ratio and diffusion activation energy calculations

3.1 Intrinsic diffusivities ratio of Cu and Al analysis

We can analyse described the experimental results in the Al-Cu system for bulk samples [19] since the ratio D_{Al}^*/D_{Cu}^* was not calculated in [19]:

$$\frac{D_{Cu}^*}{D_{Al}^*} \approx \frac{\sum_{j=1}^N X_j - X_K(1 - C_i)\sqrt{\pi}}{\sum_{j=1}^N X_j + C_i X_K \sqrt{\pi}} < 1, C_i = C_{Al}, \quad (25)$$

where N is formed phases quantity, X_j is phase j 's thickness, C_i is the average concentration of aluminium in phase i , and X_K is the Kirkendall shift length.

Five phases are formed in the Al-Cu system at temperatures from 400 to 535°C in bulk samples [19]: θ -phase (phase 1) CuAl_2 ($C_1 = 2/3$), η_2 -phase (phase 2) CuAl ($C_2 = 1/2$), ζ_2 -phase (phase 3b) Cu_4Al_3 ($C_{3b} = 3/7$), δ -phase (phase 3a) Cu_3Al_2 ($C_{3a} = 2/5$), and γ_2 -phase (phase 3) Cu_9Al_4 ($C_3 = 4/13 \approx 0.31 \approx 1/3$, $C = C_{Al}$). Inert markers were in δ -phase (phase 3a) Cu_3Al_2 ($C_{3a} = 2/5 = 0.4$) and moved to Al side during mutual diffusion. In general, inert markers move to the faster diffusivity component side. We can calculate ($C_{3a} = 0.4$):

$$\frac{D_{Cu}^*}{D_{Al}^*}(T_1 = 535^\circ\text{C}) \approx \frac{X_1 + X_2 + X_{3b} + X_{3a} + X_3 - X_K 0.6\sqrt{\pi}}{X_1 + X_2 + X_{3b} + X_{3a} + X_3 + 0.4X_K \sqrt{\pi}} \approx 0.814; \quad (26)$$

$$y_1 = \frac{D_{Al}^*}{D_{Cu}^*} = \frac{1}{0.814} \approx 1.228,$$

$$T_1 = 535^\circ\text{C} = 808 \text{ K}, t = 40 \text{ h}, X_K \approx 20.5 \text{ } \mu\text{m}, X_1 + X_2 + X_{3b} + X_{3a} + X_3 \approx 180 \text{ } \mu\text{m};$$

$$\frac{D_{Cu}^*}{D_{Al}^*}(T_2 = 515^\circ\text{C}) \approx \frac{X_1 + X_2 + X_{3b} + X_{3a} + X_3 - X_K(1 - C_{3a})\sqrt{\pi}}{X_1 + X_2 + X_{3b} + X_{3a} + X_3 + C_{3a}X_K \sqrt{\pi}} \approx 0.856; \quad (27)$$

$$y_2 = \frac{D_{Al}^*}{D_{Cu}^*} \approx 1.168,$$

$$T_2 = 515^\circ\text{C} = 788 \text{ K}, t = 40 \text{ h}, X_K \approx 11 \text{ } \mu\text{m}, X_1 + X_2 + X_{3b} + X_{3a} + X_3 \approx 127 \text{ } \mu\text{m};$$

$$\frac{D_{Cu}^*}{D_{Al}^*}(T_3 = 495^\circ\text{C}) \approx \frac{X_1 + X_2 + X_{3b} + X_{3a} + X_3 - X_K 0.6\sqrt{\pi}}{X_1 + X_2 + X_{3b} + X_{3a} + X_3 + 0.4X_K \sqrt{\pi}} \approx 0.916; \quad (28)$$

$$y_3 = \frac{1}{0.916} \approx 1.092,$$

$$T_3 = 495^\circ\text{C} = 768 \text{ K}, t = 40 \text{ h}, X_K \approx 5 \text{ } \mu\text{m}, X_1 + X_2 + X_{3b} + X_{3a} + X_3 \approx 101 \text{ } \mu\text{m};$$

$$\frac{D_{Cu}^*}{D_{Al}^*}(T_4 = 475^\circ\text{C}) \approx \frac{X_1 + X_2 + X_{3b} + X_{3a} + X_3 - X_K(1 - 0.4)\sqrt{\pi}}{X_1 + X_2 + X_{3b} + X_{3a} + X_3 + 0.4CX_K \sqrt{\pi}} \approx 0.969; \quad (29)$$

$$y_4 = \frac{D_{Al}^*}{D_{Cu}^*} \approx 1.032,$$

$$T_4 = 475^\circ\text{C} = 748 \text{ K}, t = 90 \text{ h}, X_K \approx 2 \text{ } \mu\text{m}, X_1 + X_2 + X_{3b} + X_{3a} + X_3 \approx 113 \text{ } \mu\text{m}.$$

We can use these four points to calculate by the least square method to increase calculation precise:

$$\Delta Q = Q_{Al} - Q_{Cu} = \frac{4 \sum_{j=1}^4 \left(\frac{1000}{RT_j} \ln y_j \right) - \sum_{j=1}^4 \ln y_j \sum_{j=1}^4 \frac{1000}{RT_j}}{4 \sum_{j=1}^4 \left(\frac{1000}{RT_j} \right)^2 - \left(\sum_{j=1}^4 \frac{1000}{RT_j} \right)^2} \approx -13.4 \text{ kJ/mol}, \quad (30)$$

$$y_0 = \exp \frac{\sum_{j=1}^4 \left(\frac{1000}{RT_j} \right)^2 \sum_{j=1}^4 \ln y_j - \sum_{j=1}^4 \frac{1000}{RT_j} \sum_{j=1}^4 \left(\frac{1000}{RT_j} \ln y_j \right)}{4 \sum_{j=1}^4 \left(\frac{1000}{RT_j} \right)^2 - \left(\sum_{j=1}^4 \frac{1000}{RT_j} \right)^2} \approx \exp(2.2) \approx 9, \quad (31)$$

$$\frac{D_{Al}^*}{D_{Cu}^*}(T) = \frac{D_{0Al}^*}{D_{0Cu}^*} e^{(Q_{Al}-Q_{Cu})/(RT)} \approx 9e^{-13.4 \text{ kJmol}^{-1}/(RT)}, \quad (32)$$

$$\frac{D_{Al}^*}{D_{Cu}^*}(T_5) = y_5 = 1 \Rightarrow T_5 = \frac{13400 \text{ J/mol}}{R \ln 9} \approx 733 \text{ K} \approx 460^\circ \text{C}, \quad (33)$$

so $Q_{Al} < Q_{Cu}$ ($Q_{Al}-Q_{Cu} = -13.4 \text{ kJ/mol}$) because the Cu^{2+} ions have less mobilities than the Al^{3+} ions, and we can conclude that the Kirkendall displacement changes sign at a temperature about $T_5 \approx 460^\circ \text{C}$ for bulk samples. The pre-exponential factors are different in nine times: $D_{0Al}^* \approx 9D_{0Cu}^*$.

Diffusion activation energy of Al is less than the diffusion activation energy of Cu ($Q_{Al} < Q_{Cu}$) at temperatures from $160\text{--}250^\circ \text{C}$ for mutual diffusion in copper-aluminium thin film double layers, but the pre-exponential factors are different in 10 times [9]. Isolated W islands, 150 \AA in diameter, have been deposited between Cu and Al thin film double layers to serve as inert diffusion markers. Marker displacements have been measured. We can calculate the ratio D_{Al}^*/D_{Cu}^* for each phase at different temperatures:

$$\begin{aligned} \frac{D_{Cu}^*}{D_{Al}^*}(T) &= \frac{D_{0Cu}^*}{D_{0Al}^*} e^{(Q_{Al}-Q_{Cu})/(RT)} = 24e^{-14 \text{ kJmol}^{-1}/(RT)} \text{ in } \theta\text{-phase (phase 1) CuAl}_2, C_{Al} \\ &= 2/3 \approx 0.67, \end{aligned}$$

$$\frac{D_{1Cu}^*}{D_{1Al}^*}(T = 250^\circ \text{C} = 523 \text{ K}) = 24e^{-14000 \text{ Jmol}^{-1}/(8.314 \times 523)} \approx 24e^{-3.22} \approx 0.96,$$

$$\frac{D_{1Cu}^*}{D_{1Al}^*}(T = 160^\circ \text{C} = 433 \text{ K}) \approx 24e^{-3.89} \approx 0.49,$$

so the Al atoms diffuse faster than the Cu atoms in θ -phase at temperatures from 160 to 250°C ;

$$\begin{aligned} \frac{D_{Cu}^*}{D_{Al}^*}(T) &= \frac{D_{0Cu}^*}{D_{0Al}^*} e^{(Q_{Al}-Q_{Cu})/(RT)} = 7 \cdot 10^4 e^{-38 \text{ kJmol}^{-1}/(RT)} \text{ in } \eta_2\text{-phase (phase 2) CuAl}, C_{Al} \\ &= 1/2 = 0.5, \end{aligned}$$

$$\frac{D_{2Cu}^*}{D_{2Al}^*}(T = 250^\circ \text{C}) = 7 \cdot 10^4 e^{-38000 \text{ Jmol}^{-1}/(RT)} \approx 11.2, \quad \frac{D_{2Cu}^*}{D_{2Al}^*}(T = 160^\circ \text{C}) \approx 1.8,$$

so the Cu atoms diffuse faster than the Al atoms in η_2 -phase at temperatures from 160 to 250°C ;

$$\frac{D_{Cu}^*}{D_{Al}^*}(T) = \frac{D_{0Cu}^*}{D_{0Al}^*} e^{(Q_{Al}-Q_{Cu})/(RT)} = 14e^{-9kJmol^{-1}/(RT)} \text{ in } \gamma_2\text{-phase (phase 3) Cu}_9\text{Al}_4, C_{Al}$$

$$= 4/13 \approx 0.31,$$

$$\frac{D_{3Cu}^*}{D_{3Al}^*}(T = 250^\circ C) = 14e^{-9000Jmol^{-1}/(RT)} \approx 1.77, \frac{D_{3Cu}^*}{D_{3Al}^*}(T = 160^\circ C)$$

$$= 14e^{-9kJmol^{-1}/(RT)} \approx 1.15,$$

so the Cu atoms diffuse faster than the Al atoms in γ_2 -phase at temperatures from 160 to 250°C.

The Cu-rich phases can be formed faster than the Al-rich phases at temperatures from 160 to 250°C, and the Cu atoms can diffuse faster than the Al atoms in the Al-Cu system at temperatures from 160 to 250°C. The Al-rich phases can be formed faster than the Cu-rich phases at temperatures from 400 to 535°C, and the Al atoms can diffuse faster than the Cu atoms in the Al-Cu system at temperatures from 400 to 535°C. It depends on the crystal structure of each phase, but, in general, it could depends on conclusions that the Cu^{2+} ions are less mobile than the Cu^+ ions, and the ratio D_{Al}^*/D_{Cu}^* depends on temperature.

3.2 Diffusion activation energy calculation

3.2.1 Diffusion activation energy calculation in the Cu-Al system

Mutual diffusion coefficients were calculated for all five phases [19]:

$$\tilde{D}_1^* = 5.6 \cdot 10^{-5} e^{-127.6kJmol^{-1}/(RT)} m^2/s; \tilde{D}_2^* = 2.2 \cdot 10^{-4} e^{-148.5kJmol^{-1}/(RT)} m^2/s; \quad (34)$$

$$\tilde{D}_{3b}^* = 1.6 \cdot 10^2 e^{-230.5kJmol^{-1}/(RT)} m^2/s, \tilde{D}_{3a}^* = 2.1 \cdot 10^{-4} e^{-138.1kJmol^{-1}/(RT)} m^2/s, \tilde{D}_3^*$$

$$= 8.5 \cdot 10^{-5} e^{-136kJmol^{-1}/(RT)} m^2/s.$$

We can see that $Q_1 < Q_2$, $Q_1 < Q_3$, and $Q_3 < Q_2$ because of $K_1 > K_2$, $K_1 > K_3$, and $K_3 > K_2$, and $D_{01} \approx D_{02} \approx D_{03}$. Phase j 's rate formation is K_j . Three phases are formed in the Al-Cu system at temperatures 300 and 350°C [5]: $CuAl_2$, $CuAl$, and Cu_9Al_4 . Phases formation rates were experimentally measured: $K_1 = 860 \times 10^{-18} m^2/s$, $K_2 = 100 \times 10^{-18} m^2/s$, and $K_3 = 360 \times 10^{-18} m^2/s$ at temperature 350°C; $K_1 = 77 \times 10^{-18} m^2/s$, $K_2 = 18 \times 10^{-18} m^2/s$, and $K_3 = 35 \times 10^{-18} m^2/s$ at temperature 300°C, so $K_1 > K_2$, $K_1 > K_3$, and $K_3 > K_2$. We can calculate assuming $C_1 = 2/3$, $C_2 = 1/2$, $C_3 = 1/3$, $C = C_{Al}$ [11]:

$$D_1 \approx \frac{1}{2} \left(C_1(1 - C_1)K_1 + C_2(1 - C_1)\sqrt{K_1K_2} + C_3(1 - C_1)\sqrt{K_1K_3} \right); \quad (35)$$

$$D_2 \approx \frac{1}{2} \left(C_2(1 - C_2)K_2 + C_1(1 - C_2)\sqrt{K_1K_2} + C_3(1 - C_2)\sqrt{K_2K_3} \right); \quad (36)$$

$$D_3 \approx \frac{1}{2} \left(C_3(1 - C_3)K_3 + C_1(1 - C_3)\sqrt{K_1K_3} + C_2(1 - C_3)\sqrt{K_2K_3} \right); \quad (37)$$

$$D_1(T_2 = 350^\circ C) \approx \frac{1}{9}K_1 + \frac{1}{12}\sqrt{K_1K_2} + \frac{1}{18}\sqrt{K_1K_3} \approx 150$$

$$\cdot 10^{-18} m^2/s, D_1(T_1 = 300^\circ C) \approx 15 \cdot 10^{-18} m^2/s; \quad (38)$$

$$D_2(T_2 = 350^\circ\text{C}) \approx \frac{1}{8}K_2 + \frac{1}{12}\sqrt{K_1K_2} + \frac{1}{12}\sqrt{K_2K_3} \approx 50 \times 10^{-18} \text{ m}^2/\text{s}, D_2(T_1 = 300^\circ\text{C}) \approx 8 \cdot 10^{-18} \text{ m}^2/\text{s}; \quad (39)$$

$$D_3(T_2 = 350^\circ\text{C}) \approx \frac{1}{9}K_3 + \frac{1}{18}\sqrt{K_1K_3} + \frac{1}{12}\sqrt{K_2K_3} \approx 90 \cdot 10^{-18} \text{ m}^2/\text{s}, D_3(T_1 = 300^\circ\text{C}) \approx 12 \cdot 10^{-18} \text{ m}^2/\text{s}. \quad (40)$$

Moisy et al. [5] did not calculate diffusion activation energies and the pre-exponential factors, so we can do it:

$$Q_i = \frac{RT_1T_2}{T_2 - T_1} \ln \left(\frac{D_i(T_2)}{D_i(T_1)} \right), D_{0i} = D_i(T_1)e^{Q_i/(RT_1)} = D_i(T_2)e^{Q_i/(RT_2)}; \quad (41)$$

$$\tilde{D}_1 = 4.3 \cdot 10^{-5} e^{-136.7 \text{ kJ mol}^{-1}/(RT)} \text{ m}^2/\text{s}, \tilde{D}_2 = 6.6 \cdot 10^{-8} e^{-108.8 \text{ kJ mol}^{-1}/(RT)} \text{ m}^2/\text{s}, \quad (42)$$

$$\tilde{D}_3 = 9.6 \cdot 10^{-7} e^{-119.6 \text{ kJ mol}^{-1}/(RT)} \text{ m}^2/\text{s}.$$

Eq. (42) correspond to Eq. (34). We can use several, N , points to calculate by the least square method to increase calculation precise:

$$Q_i = - \frac{N \sum_{j=1}^N \left(\frac{1000}{RT_j} \ln D_i(T_j) \right) - \sum_{j=1}^N \ln D_i(T_j) \sum_{j=1}^N \frac{1000}{RT_j}}{N \sum_{j=1}^N \left(\frac{1000}{RT_j} \right)^2 - \left(\sum_{j=1}^N \frac{1000}{RT_j} \right)^2} [\text{kJ/mol}], \quad (43)$$

$$D_{0i} = \exp \frac{\sum_{j=1}^5 \left(\frac{1000}{RT_j} \right)^2 \sum_{j=1}^5 \ln D_i(T_j) - \sum_{j=1}^5 \frac{1000}{RT_j} \sum_{j=1}^4 \left(\frac{1000}{RT_j} \ln D_i(T_j) \right)}{5 \sum_{j=1}^5 \left(\frac{1000}{RT_j} \right)^2 - \left(\sum_{j=1}^5 \frac{1000}{RT_j} \right)^2} [\text{m}^2/\text{s}]. \quad (44)$$

Eqs. (43) and (44) give Eq. (41) for only two points ($N = 2$).

3.2.2 Diffusion activation energy calculation in pure iron

A method of dislocation pipe diffusion parameter determination during the type B diffusion kinetics was suggested by the model of dislocation pipe diffusion involving outflow [6, 20]. The method involves diffusion dislocation pipe kinetics for two different annealing times at the same temperature during the type B kinetics and dislocation pipe kinetics for one annealing time at other lower temperature during the type C kinetics. Transition time for type B kinetics to type A kinetics (volume diffusion) and kinetics law $t^{1/6}$ [7] for cone top rate are used in this method.

Bulk diffusion coefficients, D_V , for the diffusion of ^{59}Fe in the high-purity iron were calculated in [21] using type B \rightarrow A kinetics: $D_V = 1.5 \cdot 10^{-18} \text{ m}^2 \text{ s}^{-1}$ at $T_1 = 973 \text{ K}$ for $t_B \rightarrow A = 67.5 \text{ ks}$ ($T_m/T_1 = 1.86$, T_m is melting point of iron). Only one experiment was carried out at the same temperature for two annealing times t_1 and t_2 ($t_1 < t_2$, $t_2 = 40 t_1$). Dislocation diffusion coefficients for the diffusion of ^{59}Fe in the iron were calculated in [21] using type C kinetics: $D_d = 3 \cdot 10^{-16} \text{ m}^2 \text{ s}^{-1}$ at $T_2 = 753 \text{ K}$ for $t_C = 2.4 \text{ ks}$ ($T_m/T_2 = 2.4$). One can find ratio $D_d/D_V: y(t_{C \rightarrow B}) = \sqrt{\frac{D_d}{6D}} \delta$, where $\delta = 1 \text{ nm}$, $\frac{D_d}{D} = 4.3 \times 10^6$. Ratio D_d/D_V increases remarkably for lower temperature. Dislocation

pipe and volume diffusion activation energies and pre-exponential factors were not calculated in [21]. It is possible to calculate E_d and D_0 : $E_d = \ln \left(\frac{D_d(T_1)}{D_d(T_2)} \right) k_B \frac{T_1 T_2}{T_1 - T_2}$, $D_0 = D_d(T_1) \exp \left(\frac{E_d}{k_B T_1} \right)$, $E_d = 1.1 \text{ eV}$; $Q_d = 106 \text{ kJ/mol}$, $D_0 = 6.85 \cdot 10^{-9} \text{ m}^2 \text{ s}^{-1}$. One can calculate dislocation pipe diffusion coefficient for temperature 973 K directly ($T_1 = 753 \text{ K}$ and $T_2 = 693 \text{ K}$ (type C kinetics)): $D_d \approx 10^{-14} \text{ m}^2 \text{ s}^{-1}$. Such value corresponds to value calculated using the proposed method. The Fisher law ($t^{1/4}$) gives $D_d \approx 10^{-16} \div 10^{-15} \text{ m}^2 \text{ s}^{-1}$. Such value is in two orders lower than experimentally obtained in [21]. The volume diffusion activation energy E_V can be calculated: $E_V = \ln \left(\frac{D_0}{D_V(T_1)} \right) k_B T_1$, $E_V = 1.85 \text{ eV}$; $Q_V \approx 179 \text{ kJ/mol}$. Ratio $\frac{E_d}{E_V} = 0.6$ as described in [8].

4. Conclusions

The Al atoms diffuse faster than the Cu atoms at a temperature higher than 475°C, but the Cu atoms diffuse faster than the Al atoms at a temperature lower than 100°C. The diffusion activation energy of Al is less than the diffusion activation energy of Cu at a temperature higher than 475°C, but diffusion activation energy of Cu is less than the diffusion activation energy of Al at a temperature lower than 100°C. Our investigations show that it is possible because the Cu^{2+} ions are less mobile than Cu^+ ions.

Volume diffusion activation energy of Fe is higher than volume diffusion activation energy of Cu or Al, but dislocation pipe diffusion activation energy of Fe is smaller than volume diffusion activation energy of Cu or Al, so the Fe atoms diffuse faster along the dislocation line, but the Cu or Al atoms diffuse faster in volume.


Author details

Mykhaylo Viktorovych Yarmolenko

Faculty of Market, Information and Innovation Technologies, Kyiv National University of Technologies and Design, Cherkasy, Ukraine

*Address all correspondence to: yarmolenko.mv@knuutd.edu.ua

IntechOpen

© 2021 The Author(s). Licensee IntechOpen. This chapter is distributed under the terms of the Creative Commons Attribution License (<http://creativecommons.org/licenses/by/3.0>), which permits unrestricted use, distribution, and reproduction in any medium, provided the original work is properly cited. 

References

- [1] Kizaki T, Minho O, Kajihara M. Rate-controlling process of compound growth in Cu-Clad Al wire during isothermal annealing at 483–543 K. *Materials Transactions*. 2020;**61**(1): 188-194. DOI: 10.2320/matertrans.MT-M2019207
- [2] Braunovic M, Alexandrov N. Intermetallic compounds at aluminum-to-copper electrical interfaces: Effect of temperature and electric current. *IEEE Transactions on Components, Packaging, and Manufacturing Technology: Part A*. 1994;**17**(1):78-85. DOI: 10.1109/95.296372
- [3] Goh CS, Chong WLE, Lee TK, Breach C. Corrosion study and intermetallics formation in gold and copper wire bonding in microelectronics packaging. *Crystals*. 2013;**3**(3):391-404. DOI: 10.3390/cryst3030391
- [4] Yarmolenko MV. Copper and aluminum electric corrosion investigation and intermetallics disappearance in Cu-Al system analysis. *Phys. Chem. Solid St.* 2020;**21**(2): 294-299. <https://journals.pnu.edu.ua/index.php/pcss/article/view/3055>
- [5] Moisy F, Sauvage X, Hug E. Investigation of the early stage of reactive interdiffusion in the Cu-Al system by *in-situ* transmission electron microscopy. *Materialia*. 2020;**9**:100633. DOI: 10.1016/j.mtla.2020.100633
- [6] Yarmolenko MV. Method of dislocation and bulk diffusion parameters determination. *Metallofizika i Noveishie Tekhnologii*. 2020;**42**(11): 1537-1546. <https://mfint.imp.kiev.ua/article/v42/i11/MFiNT.42.1537.pdf>
- [7] Yarmolenko MV. Intermediate phase cone growth kinetics along dislocation pipes inside polycrystal grains. *AIP Advances*. 2018;**8**:095202. DOI: 10.1063/1.5041728
- [8] Mehrer H. *Diffusion in Solids*. New York: Springer; 2007. 651p. http://users.ensc.concordia.ca/~tmg/images/7/79/Diffusion_in_solids_Helmut_Mehrer.pdf
- [9] Hentzell HTG, Tu KN. Interdiffusion in copper–aluminum thin film bilayers. II. Analysis of marker motion during sequential compound formation. *Journal of Applied Physics*. 1983;**54**:6929-6937. DOI: 10.1063/1.332000
- [10] Darken LS. Diffusion, mobility and their interrelation through free energy in binary metallic systems. *Transactions AIME*. 1948;**175**:184-201. <http://garfield.library.upenn.edu/classics1979/A1979HJ27500001.pdf>
- [11] Yarmolenko MV. Intermetallics disappearance rate analysis in double multiphase systems. *DDF*. 2021;**407**: 68-86. DOI: 10.4028/www.scientific.net/ddf.407.68
- [12] Włodarczyk PP, Włodarczyk B. Effect of hydrogen and absence of passive layer on corrosive properties of aluminium alloys. *Materials*. 2020;**13**(7): 1580-1593. DOI: 10.3390/ma13071580
- [13] Kumar S, Handwerker CA, Dayananda MA. Intrinsic and interdiffusion in Cu-Sn system. *JPEDAV*. 2011;**32**:309-319. DOI: 10.1007/s11669-011-9907-91547-7037
- [14] Tu KN. *Electronic Thin-Film Reliability*. 1st ed. New York: Cambridge University Press; 2010. 392p. DOI: https://www.amazon.com/Electronic-Thin-Film-Reliability-King-Ning-Tu-ebook-dp-B00QIT3LXA/dp/B00QIT3LXA/ref=mt_other?_encoding=UTF8&me=&qid=
- [15] Epishin A, Chyrkin A, Camin B, Saillard R, Gouy S, Viguiet B. Interdiffusion in CMSX-4 related Ni-base alloy system at a supersolvus

temperature. DDF. 2021;**407**:1-10. DOI: 10.4028/www.scientific.net/ddf.407.1

[16] Prawoto Y. Synergy of erosion and galvanic effects of dissimilar steel welding: Field failure analysis case study and laboratory test results. Journal of King Saud University – Engineering Sciences. 2013;**25**:59-64. DOI: 10.1016/j.jksues.2011.12.001

[17] Yarmolenko MV. Intrinsic diffusivities ratio analysis in the Al-Cu system. Phys. Chem. Solid St. 2020; **21**(4):720-726. <https://journals.pnu.edu.ua/index.php/pcss/article/view/4440>

[18] Yarmolenko MV. Intermetallics disappearance rates and intrinsic diffusivities ratios analysis in the Cu-Zn and the Cu-Sn systems. Phys. Chem. Solid St. 2021;**22**(1):80-87. <https://journals.pnu.edu.ua/index.php/pcss/article/view/4744>

[19] Funamizu Y, Watanabe K. Interdiffusion in the Al-Cu system. Transactions of the Japan Institute of Metals. 1971;**12**(3):147-152. DOI: 10.2320/matertrans1960.12.147

[20] Yarmolenko MV. Analytically solvable differential diffusion equations describing the intermediate phase growth. Metallofizika i Noveishie Tekhnologii. 2018;**40**(9):1201-1207. <https://mfint.imp.kiev.ua/article/v40/i09/MFiNT.40.1201.pdf>

[21] Shima Y, Ishikawa Y, Nitta H, Yamazaki Y, Mimura K, Isshiki M, et al. Self-diffusion along dislocations in ultra high purity iron. Materials Transactions. 2002;**43**(2):173-177. <https://www.jim.or.jp/journal/e/43/02/173.html>